JOURNAL OF GUIDANCE, CONTROL, AND DYNAMICS
Vol. 19, No. 1, January–February 1996

General Formulation for N-Body Tethered Satellite System Dynamics

M. Keshmiri* and A. K. Misra†
McGill University, Montreal, Quebec H3A 2K6, Canada
and
V. J. Modi‡
University of British Columbia, Vancouver, British Columbia V6T 1Z4, Canada

General three-dimensional motion of tethered N-body systems is considered. Equations of motion are derived using the Lagrangian formulation. The derived equations are valid for large librational motion, variable lengths, and an arbitrary orbit. The elasticity and mass of the tethers are taken into account. Longitudinal and transverse displacements of the tethers are assumed to be small compared to the lengths and are discretized using the assumed-mode method. The nonlinear equations of motion are used for simulation of the system dynamics. For eigenvalue analysis and control applications, however, the equations need to be linearized; this is done analytically. Several examples are considered. Librational as well as longitudinal and transverse elastic frequencies of several multibody systems are obtained. A segmented-tether model is used to obtain the higher frequencies of a system. It is observed that the frequencies associated with the in-plane and out-of-plane motion of the system, ω_I and ω_O, are related by $(\omega_O/\Omega_c)_j^2 \approx (\omega_I/\Omega_c)_j^2 + 1$, where Ω_c is the orbital frequency. Typical transient responses of three-body and four-body tethered systems are obtained.

Introduction

TETHERED satellite systems (TSS) have received a lot of attention in recent years. There have been many investigations on their dynamics and control.[1–3] Since initially the proposed applications involved only two bodies, until recent years, the interest of the investigators was focused on two-body systems. There have been several proposals recently, however, to use multibody tethered systems, such as the space-station-based microgravity laboratory that has been proposed by some potential users.

The in-plane dynamics of three-body TSS has been studied by Lorenzini,[4] as well as by Misra et al.,[5] using different approaches. Lorenzini et al.[6] and Cosmo et al.[7] have also studied the dynamics of the four-mass tethered system called the tether elevator/crawler system (TECS); the former is based on a bead model and Newtonian approach, whereas the latter uses a Lagrangian approach to study the in-plane dynamics. The in-plane eigenvalues and eigenvectors for the four-body system were presented by Cosmo et al.[7]; in addition, damping of librational and longitudinal oscillations were also considered. Kumar et al.[8] have attempted to conduct a fairly basic study of in-plane transverse oscillations of three-body, two-tethered systems. A fairly general model for librational dynamics of N-body TSS has been formulated by Misra and Modi,[9] ignoring mass and elasticity of the tethers. It has been shown that the flexibility of tethers plays an important role in the stability of a TSS subjected to aerodynamic forces.[10,11] Thus, it should be included in a general model.

The objective of this paper is to develop a formulation for simulation of the three-dimensional nonlinear dynamics of N-body systems with flexible tethers using a continuum model and to derive, subsequently, the linearized equations of motion for control and linear stability analysis purposes. Stationkeeping phase is treated as a special case of the variable length case, where the tether lengths are constant.

Received March 17, 1994; revision received July 14, 1995; accepted for publication July 18, 1995.

*Graduate Student, Department of Mechanical Engineering.
†Professor, Department of Mechanical Engineering. Associate Fellow AIAA.
‡Professor, Department of Mechanical Engineering, 2324 Main Mall. Fellow AIAA.

Formulation of the Problem

Kinematics and Energy Expressions

The system under consideration, Fig. 1, consists of N bodies connected by $N-1$ tethers. The former are assumed to be point masses, having masses $m_i, i = 1, 2, \ldots, N$. The tethers have mass densities (mass/length) $\rho_i, i = 1, 2, \ldots, N-1$, and they are considered as elastic. The ith tether, having length ℓ_i, connects the masses m_i

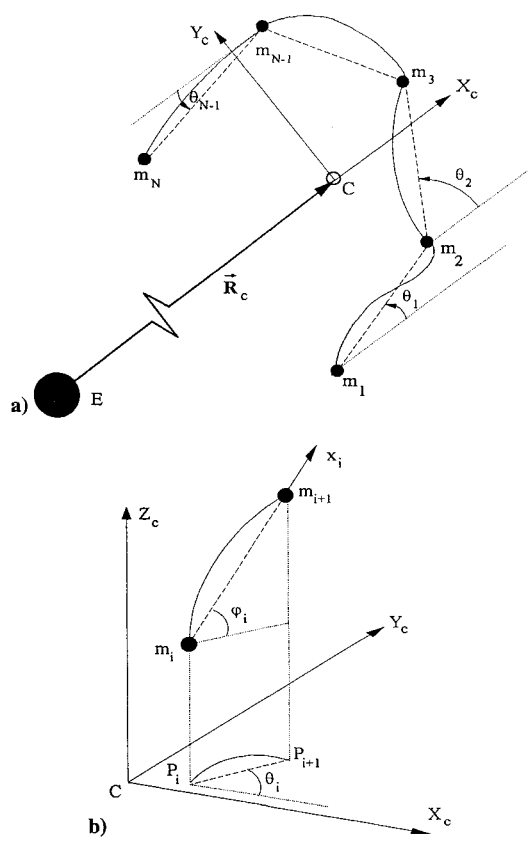

Fig. 1 Geometry of the system: a) projection of the N-body system in the orbital plane and b) definition of angles θ_i and ϕ_i.

and m_{i+1}. To have a more general model and include systems with crawlers, it is assumed that every tether is reeled partially by the corresponding end bodies. Tether i is reeled out at a rate of $\rho_i \alpha_i \dot{\ell}_i$ from body i and reeled in at a rate of $\rho_i \beta_i \dot{\ell}_i$ to body $i+1$. It follows that the rate of change of mass of body i is given by

$$\dot{m}_i = \rho_{i-1}\beta_{i-1}\dot{\ell}_{i-1} - \rho_i \alpha_i \dot{\ell}_i \tag{1}$$

whereas $\alpha_i - \beta_i = 1$. Dimensionless coefficients α_i and β_i can be either positive or negative and, in general, they are functions of time.

The motion of the system is described with respect to an orbital coordinate system X_c, Y_c, Z_c with unit vectors $\hat{i}_c, \hat{j}_c, \hat{k}_c$ and its origin at the instantaneous center of mass of the system. The X_c axis is along the local vertical, the Z_c axis is along the orbit normal, and the Y_c axis completes the right-hand triad. The orbit is assumed to be Keplerian with instantaneous angular velocity $\dot{\psi} = \Omega_c$. For a circular orbit, of course, Ω_c is a constant. In addition to the orbital coordinate system, a tether coordinate system corresponding to each tether, x_i, y_i, z_i, $i = 1, 2, \ldots, N-1$, where the x_i axis is along the connection line of the two ends of the tether, is used to describe the motion of the system. The orientation of this coordinate system with respect to the orbital coordinate system is defined by θ_i and ϕ_i, the in-plane and out-of-plane librational angles of the line of connection already mentioned. Vectors $\hat{i}_i, \hat{j}_i$, and $\hat{k}_i$ represent unit vectors along this system of coordinate axes.

Let us define $\boldsymbol{R}_i$ and $\boldsymbol{R}_{t_i}$ as the position vectors of the ith body and an element of the ith tether with respect to the center of mass of the system, respectively. Also let us define $\boldsymbol{r}_i$ and $\boldsymbol{r}_{t_i}$ as the displacement vectors of body $i+1$ and an element of the ith tether with respect to body i. From the definition of the center of mass that is assumed to move in a Keplerian orbit one gets the following constraint relation between the position vectors:

$$\sum_{i=1}^{N} m_i \boldsymbol{R}_i + \sum_{i=1}^{N-1} \rho_i \int_0^{\ell_i} \boldsymbol{R}_{t_i}\, \mathrm{d}x_i = \boldsymbol{0} \tag{2}$$

Substituting

$$\boldsymbol{R}_i = \boldsymbol{R}_1 + \sum_{j=1}^{i-1} \boldsymbol{r}_j, \qquad \boldsymbol{R}_{t_i} = \boldsymbol{R}_i + \boldsymbol{r}_{t_i} \tag{3}$$

in Eq. (2), and performing some algebra, one obtains

$$\boldsymbol{R}_k = \sum_{j=1}^{N-1} (A_{kj}\boldsymbol{r}_j - \bar{\mu}_j \boldsymbol{b}_j) \tag{4}$$

where

$$\boldsymbol{b}_i = \frac{1}{\ell_0}\int_0^{\ell_i} \boldsymbol{r}_{t_i}\, \mathrm{d}x_i$$

The mass coefficients in Eq. (4) are defined as

$$A_{kj} = B_j - H(j-k), \qquad \bar{\mu}_j = \rho_j \ell_0 / m \tag{5}$$

where

$$B_j = \sum_{i=1}^{j} \mu_i, \qquad \mu_i = \frac{m_i + \bar{m}_i}{m}, \qquad \bar{m}_i = \rho_i \ell_i \tag{6}$$

and ℓ_0 is a reference length, m is total mass, and H is the Heaviside step function. Since ℓ_i, in general, is a function of time, it is clear that μ_i is time dependent; however, $\bar{\mu}_j$ is a constant.

Using Eqs. (4) and (5) and the fact that the time derivatives of the mass coefficients A_{ij} are the same as those of B_j, the velocity and acceleration of the ith mass are given by

$$\begin{aligned} \dot{\boldsymbol{R}}_i &= \sum_{j=1}^{N-1} (\dot{B}_j \boldsymbol{r}_j + A_{ij}\dot{\boldsymbol{r}}_j - \bar{\mu}_j \dot{\boldsymbol{b}}_j) \\ \ddot{\boldsymbol{R}}_i &= \sum_{j=1}^{N-1} (\ddot{B}_j \boldsymbol{r}_j + 2\dot{B}_j \dot{\boldsymbol{r}}_j + A_{ij}\ddot{\boldsymbol{r}}_j - \bar{\mu}_j \ddot{\boldsymbol{b}}_j) \end{aligned} \tag{7}$$

where $\dot{B}_j = -\rho_j \beta_j \dot{\ell}_j / m$ and

$$\dot{\boldsymbol{r}}_j = \mathring{\boldsymbol{r}}_j + \boldsymbol{\Omega}_j \times \boldsymbol{r}_j, \qquad \dot{\boldsymbol{b}}_j = \mathring{\boldsymbol{b}}_j + \boldsymbol{\Omega}_j \times \boldsymbol{b}_j \tag{8}$$

Here $(\mathring{})$ represents the time derivative of the vector with respect to the tether coordinate frame and $\boldsymbol{\Omega}_j$ is the angular velocity of the jth tether with respect to the inertial frame.

Derivation of the equations of motion can be carried out using various approaches. Here Lagrange's equations are used. Thus, expressions for the kinetic and potential energy must be written first. It is assumed here that the orbital motion of the system is not affected by its attitude dynamics. Therefore, only the attitude kinetic and potential energies are required to obtain the equations of motion corresponding to the attitude dynamics of the system.

Attitude kinetic energy of the system is given by

$$T_{\text{att}} = \sum_{i=1}^{N} \left(\frac{1}{2} m_i \dot{\boldsymbol{R}}_i \cdot \dot{\boldsymbol{R}}_i\right) + \sum_{i=1}^{N-1} \left[\frac{1}{2}\rho_i \int_0^{\ell_i} \left(\dot{\boldsymbol{R}}_{t_i} \cdot \dot{\boldsymbol{R}}_{t_i}\right) \mathrm{d}x_i\right] \tag{9}$$

Using Leibnitz's rule of differentiation of integrals with time varying limits for $\boldsymbol{b}_i$, it can be shown that

$$\dot{\boldsymbol{b}}_i = \frac{\mathrm{d}}{\mathrm{d}t}\left(\frac{1}{\ell_0}\int_0^{\ell_i} \boldsymbol{r}_{t_i}\, \mathrm{d}x_i\right) = \frac{1}{\ell_0}\left[\int_0^{\ell_i} \dot{\boldsymbol{r}}_{t_i}\, \mathrm{d}x_i - \beta_i \dot{\ell}_i \boldsymbol{r}_i\right] \tag{10}$$

where $\dot{\boldsymbol{r}}_{t_i} = [(\partial/\partial t) + \dot{\ell}_i(\partial/\partial x_i)]\boldsymbol{r}_{t_i}$. It should be mentioned here that for the variables that are functions of time t and length coordinate x, e.g., $\boldsymbol{r}_{t_i}$ and $\boldsymbol{R}_{t_i}$, $(\dot{})$ and $(\mathring{})$ stand for total derivative (i.e., including the convective derivative) with respect to time in the inertial and local coordinate frames, respectively. Substituting for $\boldsymbol{R}_{t_i}$ from Eq. (3), using Eq. (10), and performing some algebra, we can rewrite Eq. (9) as

$$\begin{aligned} T_{\text{att}} = m\Bigg\{ &\sum_{i=1}^{N} \frac{1}{2}\mu_i \dot{\boldsymbol{R}}_i \cdot \dot{\boldsymbol{R}}_i + \sum_{i=1}^{N-1} \dot{R}_i \cdot (\bar{\mu}_i \dot{\boldsymbol{b}}_i - \dot{B}_i \boldsymbol{r}_i) \\ &+ \sum_{i=1}^{N-1} \frac{1}{2}\hat{\rho}_i \int_0^{\ell_i} \left(\dot{\boldsymbol{r}}_{t_i} \cdot \dot{\boldsymbol{r}}_{t_i}\right) \mathrm{d}x_i \Bigg\} \end{aligned} \tag{11}$$

where $\hat{\rho}_i = \rho_i / m$.

Similarly, gravitational potential energy of the system due to its attitude motion is given by

$$\begin{aligned} U_{g_{\text{att}}} = m\alpha_0 \Bigg\{ &\sum_{i=1}^{N} \frac{1}{2}\mu_i [\boldsymbol{R}_i - 3(\hat{\boldsymbol{I}}_c \cdot \boldsymbol{R}_i)\hat{\boldsymbol{i}}_c] \cdot \boldsymbol{R}_i \\ &+ \sum_{i=1}^{N} \bar{\mu}_i [\boldsymbol{R}_i - 3(\hat{\boldsymbol{i}}_c \cdot \boldsymbol{R}_i)\hat{\boldsymbol{i}}_c] \cdot \boldsymbol{b}_i \\ &+ \sum_{i=1}^{N-1} \frac{1}{2}\hat{\rho}_i \int_0^{\ell_i} \left[\boldsymbol{r}_{t_i} - 3\left(\hat{\boldsymbol{i}}_c \cdot \boldsymbol{r}_{t_i}\right)\hat{\boldsymbol{i}}_c\right] \cdot \boldsymbol{r}_{t_i}\, \mathrm{d}x_i \Bigg\} \end{aligned} \tag{12}$$

where $\alpha_0 = GM/R_c^3$. Note that α_0 is not a constant in general. The gravity gradient effects are accounted for in the dynamical model through $U_{g_{\text{att}}}$.

Considering up to the third-order terms in the longitudinal strain in the tethers and retaining terms up to the fourth order in the elastic energy expression, the elastic potential energy of the system can be written as

$$\begin{aligned} U_e = \sum_{i=1}^{N-1} \frac{EA_i}{2} \int_0^{\ell_i} \Bigg\{ &\left(\frac{\partial u_i}{\partial x_i} + \frac{1}{2}\left[\left(\frac{\partial v_i}{\partial x_i}\right)^2 + \left(\frac{\partial w_i}{\partial x_i}\right)^2\right]\right)^2 \\ &- \left(\frac{\partial u_i}{\partial x_i}\right)^2 \left[\left(\frac{\partial v_i}{\partial x_i}\right)^2 + \left(\frac{\partial w_i}{\partial x_i}\right)^2\right] \Bigg\} \mathrm{d}x_i \end{aligned} \tag{13}$$

where u_i, v_i, and w_i are the longitudinal and transverse displacements of an element of the ith tether. These are discussed further in the following section.

Discretization and Generalized Coordinates

The elastic displacements of an element of the jth tether at a distance x_j, measured from the mass m_j along the underformed

tether, are denoted by u_j, v_j, and w_j, along x_j, y_j, and z_j, respectively. The first one is the longitudinal displacement, whereas the last two are the transverse displacements of the element. Therefore, the displacement vectors $\boldsymbol{r}_j$ and $\boldsymbol{r}_{t_j}$ can be written as

$$\boldsymbol{r}_j = (\ell_j + u_{\ell_j})\hat{\boldsymbol{i}}_j, \qquad \boldsymbol{r}_{t_j} = (x_j + u_j)\hat{\boldsymbol{i}}_j + v_j\hat{\boldsymbol{j}}_j + w_j\hat{\boldsymbol{k}}_j \tag{14}$$

where u_{ℓ_j} is the total stretch of the jth tether.

The elastic displacements, which are functions of both x_j and time t, can be expanded in terms of a set of admissible functions as follows:

$$\begin{aligned} u_j(x_j, t) &= \boldsymbol{X}_j(s_j)^T\boldsymbol{\xi}_j(t), \qquad v_j(x_j, t) = \boldsymbol{Y}_j(s_j)^T\boldsymbol{\eta}_j(t) \\ w_j(x_j, t) &= \boldsymbol{Z}_j(s_j)^T\boldsymbol{\nu}_j(t) \end{aligned} \tag{15}$$

where $s_j = x_j/\ell_j$ is a nondimensional distance, $\boldsymbol{\xi}_j$, $\boldsymbol{\eta}_j$, and $\boldsymbol{\nu}_j$ are vectors of longitudinal and transverse elastic degrees of freedom (DOF), and $\boldsymbol{X}_j$, $\boldsymbol{Y}_j$, and $\boldsymbol{Z}_j$ are column vectors containing longitudinal and transverse admissible functions corresponding to the jth tether. The admissible functions are arbitrary, but they must satisfy at least the geometric boundary conditions in an energy formulation. The following functions are chosen as admissible functions in this formulation:

$$X_{jk}(s_j) = s_j^{2k-1}, \qquad Y_{jk}(s_j) = Z_{jk}(s_j) = \sqrt{2}\sin(k\pi s_j) \tag{16}$$

In three-dimensional motion, N-point masses can have a maximum of $3N$ degrees of freedom. Confining the center of mass to a specified trajectory reduces this number to $3N-3$. Since the system under consideration consists of N-point masses connected by $N-1$ elastic tethers in a chain configuration, the motion of the system can be described by $3N-3$ rigid degrees of freedom, corresponding to the rigid body motion of the tethers, and N_e elastic degrees of freedom for all tethers.

The generalized coordinates of the system are chosen here as

$$\boldsymbol{q} = \left\{\boldsymbol{q}_1^T, \boldsymbol{q}_2^T, \ldots, \boldsymbol{q}_{N-1}^T\right\}^T \tag{17}$$

where the subset $\boldsymbol{q}_j$ is the contribution of the jth tether to the generalized coordinates vector and consists of

$$\boldsymbol{q}_j = \left\{\theta_j, \phi_j, \ell_j, \boldsymbol{\xi}_j^T, \boldsymbol{\eta}_j^T, \boldsymbol{\nu}_j^T\right\}^T \tag{18}$$

where θ_j, ϕ_j, and ℓ_j describe the rigid body motion of the jth tether, whereas $\boldsymbol{\xi}_j$, $\boldsymbol{\eta}_j$, and $\boldsymbol{\nu}_j$ describe its elastic motion.

Such a definition of the generalized coordinates leads to a very interesting characteristic of the system that helps us to reduce the effort involved in deriving the equations of motion analytically, which can be considerable otherwise. Considering the expressions for $\boldsymbol{r}_j$, $\boldsymbol{r}_{t_j}$, and $\boldsymbol{b}_j$, we can write partial derivatives of these vectors with respect to the generalized coordinates easily. Let us define ${}_pq_n$ as the pth generalized coordinate of the nth tether. Since it belongs to the nth subset of generalized coordinates, we can then write

$$\frac{\partial \boldsymbol{r}_j}{\partial {}_pq_n} = \begin{cases} 0 \\ \dfrac{\partial \boldsymbol{r}_n}{\partial {}_pq_n} \end{cases}, \qquad \frac{\partial \boldsymbol{b}_j}{\partial {}_pq_n} = \begin{cases} 0 \\ \dfrac{\partial \boldsymbol{b}_n}{\partial {}_pq_n} \end{cases}$$

$$\frac{\partial \boldsymbol{r}_{t_j}}{\partial {}_pq_n} = \begin{cases} 0 & \text{if } j \neq n \\ \dfrac{\partial \boldsymbol{r}_{tn}}{\partial {}_pq_n} & \text{if } j = n \end{cases} \tag{19}$$

Advantage of this is taken in this formulation extensively.

Equations of Motion

Having the kinetic and potential energies of the system associated with its attitude motion, we can derive the equations of motion using Lagrange's equations. Exercising care to carry out differentiation of integral terms with time-dependent limits and performing some complicated summation and algebraic manipulations, one can come up with the following form of the equations of motion for the pth generalized coordinate of the nth tether:

$$\sum_{j=1}^{N-1}\sum_{k=1}^{N-1} {}_pG_{njk} + \sum_{j=1}^{N-1} {}_pH_{nj} + \sum_{j=1}^{N-1} {}_pP_{nj} + {}_pS_n = \frac{{}_pQ_n}{m} \tag{20}$$

where ${}_pG_{njk}$ is the term associated with partial derivatives of the mass coefficients with respect to ${}_pq_n$, which is zero except for ${}_pq_n = \ell_n$, ${}_pH_{nj}$ is the term associated with time derivatives of the mass coefficients, ${}_pP_{nj}$ is the term associated with second derivatives of displacement vectors with respect to time, and ${}_pS_n$ is an integral over the nth tether. These terms are given in Appendix A. In Eq. (20) ${}_pQ_n$ is the generalized force corresponding to ${}_pq_n$, resulting from external forces other than the gravitational force, such as thrusts, aerodynamic forces, and structural damping in the tethers.

The generalized forces corresponding to structural damping of the tethers are modeled using a special form of the Rayleigh method. They are given in the following vector form:

$$\boldsymbol{Q}_D = c\frac{\partial \boldsymbol{f}_E}{\partial \boldsymbol{q}}\dot{\boldsymbol{q}} = c\frac{\partial}{\partial \boldsymbol{q}}\left(\frac{\partial U_E}{\partial \boldsymbol{q}}\right)\dot{\boldsymbol{q}} \tag{21}$$

where c is a constant selected for the desired damping ratio.

The complexity of the derived equations can be appreciated when one compares these equations with those of N-body tethered systems with rigid and massless tethers given by Misra and Modi.[9] Since the mass and flexibility of the tethers were ignored in that formulation, one can realize that ${}_pG_{njk}$, ${}_pH_{nj}$, and ${}_pS_n$ all vanish in Eq. (20) and $\bar{\mu}_n$ and $\boldsymbol{b}_n$ become zero in Eq. (A3). Therefore, the equation of motion corresponding to ${}_pq_n$ obtained by these researchers can be written simply as follows:

$$\sum_{j=1}^{N-1} {}_pP_{nj} = \frac{{}_pQ_n}{m} \tag{22}$$

where

$${}_pP_{nj} = F_{jn}[\ddot{\boldsymbol{r}}_j + \alpha_0(\boldsymbol{r}_j - 3(\hat{\boldsymbol{i}}_c \cdot \boldsymbol{r}_j)\hat{\boldsymbol{i}}_c)] \cdot \frac{\partial \boldsymbol{r}_n}{\partial {}_pq_n} \tag{23}$$

and F_{jn} is a nondimensional mass coefficient defined by

$$F_{jn} = \sum_{i=1}^{N} \mu_i A_{ij} A_{in} \tag{24}$$

The terms in Eq. (20) become simpler even with tether mass and flexibility, if it is assumed that the changes in mass of the ith tether is equal and opposite to that of body i. It means that ith tether is being reeled in/out to/from the ith body. In this case, μ_i is a constant, the first two terms in Eq. (20) become zero, and the equation of motion for ${}_pq_n$ degree of freedom is given by

$$\begin{aligned} \frac{{}_pQ_n}{m} = {}_pS_n + \sum_{j=1}^{N-1}\Bigg\{ &\left(F_{jn}\frac{\partial \boldsymbol{r}_n}{\partial {}_pq_n} + \bar{\mu}_n A_{nj}\frac{\partial \boldsymbol{b}_n}{\partial {}_pq_n}\right) \\ &\times [\ddot{\boldsymbol{r}}_j + \alpha_0(\boldsymbol{r}_j - 3(\hat{\boldsymbol{i}}_c \cdot \boldsymbol{r}_j)\hat{\boldsymbol{i}}_c)] + \left(\bar{\mu}_j A_{jn}\frac{\partial \boldsymbol{r}_n}{\partial {}_pq_n} - \bar{\mu}_j\bar{\mu}_n\frac{\partial \boldsymbol{b}_n}{\partial {}_pq_n}\right) \\ &\times [\ddot{\boldsymbol{b}}_j + \alpha_0(\boldsymbol{b}_j - 3(\hat{\boldsymbol{i}}_c \cdot \boldsymbol{b}_j)\hat{\boldsymbol{i}}_c)]\Bigg\} \end{aligned} \tag{25}$$

where ${}_pS_n$ is as given in Appendix A. It gets simplified further when the system under consideration is in the stationkeeping phase. In this situation, ${}_pL_n$ given in Appendix A vanishes and ℓ_n is not one of the generalized coordinates any more.

Equations of Motion in the Matrix Form

To simulate the equations of motion they should be written in the matrix form

$$M\ddot{\boldsymbol{q}} = \boldsymbol{f} \tag{26}$$

where the mass matrix M is a function of $\boldsymbol{q}$ and time t, whereas the force vector $\boldsymbol{f}$ is a nonlinear function of $\boldsymbol{q}$, $\dot{\boldsymbol{q}}$, and t.

Since in many practical cases $\mu_i = \text{const}$ (i.e., ith tether is being reeled in/out to/from the ith body or the system is in the stationkeeping phase), we will work with Eq. (25) instead of Eq. (20) from now

on. Clearly only those terms with second derivative of displacement vectors with respect to time contribute to the mass matrix; i.e., the mass matrix is obtained from

$$C^{pq_n} = \sum_{j=1}^{N-1} \left\{ \left(F_{jn} \frac{\partial \boldsymbol{r}_n}{\partial_p q_n} + \bar{\mu}_n A_{nj} \frac{\partial \boldsymbol{b}_n}{\partial_p q_n} \right) \cdot \ddot{\boldsymbol{r}}_j + \left(\bar{\mu}_j A_{jn} \frac{\partial \boldsymbol{r}_n}{\partial_p q_n} - \bar{\mu}_j \bar{\mu}_n \frac{\partial \boldsymbol{b}_n}{\partial_p q_n} \right) \cdot \ddot{\boldsymbol{b}}_j \right\} + \hat{\rho}_n \int_0^{\ell_n} \left(\ddot{\boldsymbol{r}}_{t_n} \cdot {}_p\boldsymbol{g}_n \right) \mathrm{d}x_n \tag{27}$$

where ${}_p\boldsymbol{g}_n = (\partial \boldsymbol{r}_{t_n}/\partial_p q_n)$ for ${}_p q_n \neq \ell_n$ and ${}_p\boldsymbol{g}_n = [(\partial \boldsymbol{r}_{t_n}/\partial \ell_n) + (\partial \boldsymbol{r}_{t_n}/\partial x_n)]$ for ${}_p q_n = \ell_n$. Since $\boldsymbol{r}_j$, $\boldsymbol{b}_j$, and $\boldsymbol{r}_{t_j}$ are only functions of $\boldsymbol{q}_j$, one can express the second time derivatives of these vectors as

$$\ddot{\boldsymbol{r}}_j = \mathcal{D}_{r_j} \ddot{\boldsymbol{q}}_j + \boldsymbol{d}_{r_j}, \qquad \ddot{\boldsymbol{b}}_j = \mathcal{D}_{b_j} \ddot{\boldsymbol{q}}_j + \boldsymbol{d}_{b_j}, \qquad \ddot{\boldsymbol{r}}_{t_j} = \mathcal{D}_{t_j} \ddot{\boldsymbol{q}}_j + \boldsymbol{d}_{t_j} \tag{28}$$

where $\mathcal{D}_{r_j}$, $\mathcal{D}_{b_j}$, and $\mathcal{D}_{t_j}$ are row matrices with vectorial elements, and $\boldsymbol{d}_{r_j}$, $\boldsymbol{d}_{b_j}$, and $\boldsymbol{d}_{t_j}$ are vectors corresponding to the jth tether. They are given in Appendix B. Using these relations and performing the required manipulations, one can write Eq. (25) as

$$\sum_{j=1}^{N-1} ({}_p\boldsymbol{M}_n)_j \, \ddot{\boldsymbol{q}}_j = {}_p f_n \tag{29}$$

where ${}_p f_n$ is the element of force vector corresponding to ${}_p q_n$ and $({}_n\boldsymbol{M}_p)_j$ is the contribution of jth tether to the corresponding row of mass matrix to ${}_p q_n$. They are not given in this paper for the sake of brevity. Equation (29) is the equation that is used to construct the mass matrix M, and force vector, $\boldsymbol{f}$ appearing in Eq. (26).

Linearization of the Equations of Motion

To analyze the stability of the system in the linear sense and to control the system using linear control laws, such as linear quadratic regulators (LQR), we need to have the linearized form of the equations of motion. Often linearization of the equations of motion is done numerically for lengthy and complicated equations. It is always preferable, however, to obtain the linearized equations analytically, because of numerical difficulty with differentiation (such as noise). Here, although we are dealing with very complicated and lengthy equations of motion, we can linearize them analytically using the fact that all of the vectors participating in the equations are functions of only their own specific set of generalized coordinates, by virtue of Eq. (19).

Thus, Eq. (26) can be written in linearized form as

$$\left[\left(\frac{\overline{\partial M}}{\partial \boldsymbol{q}} \right) \delta \boldsymbol{q} \right] \ddot{\bar{\boldsymbol{q}}} + \bar{M} \delta \ddot{\boldsymbol{q}} = \left(\frac{\overline{\partial \boldsymbol{f}}}{\partial \boldsymbol{q}} \right) \delta \boldsymbol{q} + \left(\frac{\overline{\partial \boldsymbol{f}}}{\partial \dot{\boldsymbol{q}}} \right) \delta \dot{\boldsymbol{q}} \tag{30}$$

where $\bar{}$ indicates the value of the variable in the nominal state, about which the equations are linearized, and $\delta \boldsymbol{q}$ shows the deviation of the state from the nominal state, i.e., $\boldsymbol{q} = \bar{\boldsymbol{q}} + \delta \boldsymbol{q}$. Matrices $\partial M/\partial \boldsymbol{q}$, $\partial \boldsymbol{f}/\partial \boldsymbol{q}$, and $\partial \boldsymbol{f}/\partial \dot{\boldsymbol{q}}$ are Jacobian matrices of mass matrix and force vector with respect to $\boldsymbol{q}$ and $\dot{\boldsymbol{q}}$. They are not presented here for the sake of brevity. If the equilibrium point of the system $\ddot{\boldsymbol{q}} = \dot{\boldsymbol{q}} = \boldsymbol{0}$ is chosen as the state about which linearization is carried out, then Eq. (30) can be written as

$$\bar{M} \delta \ddot{\boldsymbol{q}} = \left(\frac{\overline{\partial \boldsymbol{f}}}{\partial \boldsymbol{q}} \right) \delta \boldsymbol{q} + \left(\frac{\overline{\partial \boldsymbol{f}}}{\partial \dot{\boldsymbol{q}}} \right) \delta \dot{\boldsymbol{q}} \tag{31}$$

Numerical Results

The formulation presented in this paper was validated in two ways: by comparing the equations of motion of some simple cases with the results of a symbolic program developed by the authors using the symbolic manipulator language Maple-V and also by comparing the numerical results of some special cases with the results of other researchers. Some of the latter comparisons are presented in the following sections.

Eigenvalue Analysis: Some Examples

Results of several cases, considered by other researchers, are used to validate the formulation. Table 1 compares the in-plane, nondimensional eigenfrequencies (ω/Ω_c) of a three-body tethered system in a circular orbit and stationkeeping phase obtained by the present formulation with the results of Kumar et al.[8] The system consists of three-point masses, $m_1 = 10^5$ kg, $m_2 = 5000$ kg, and $m_3 = 10^4$ kg, the two tethers having a linear mass density of $\rho_1 = \rho_2 = 6$ kg/km, and axial stiffness $EA_1 = EA_2 = 61{,}645$ N. Three different cases of length configurations are considered, assuming $\ell_1 + \ell_2 = 10$ km.

Although the linearized in-plane motion of the system are coupled and every eigenfrequency contributes to the motion of all generalized coordinates, the coupling is fairly weak so that each frequency is associated exclusively with either one longitudinal or one of the in-plane or out-of-plane transverse modes. This is inferred by observing the corresponding eigenvector. Thus, the modes are easily identifiable and are shown by the label Type in the last column of Table 1.

Since Kumar et al.[8] did not consider longitudinal elastic oscillations of the tethers in their analysis, they have no eigenfrequencies corresponding to these modes of the system. Although the results of the present formulation are in good accord with those of Ref. 8, the differences can be explained: ignoring the longitudinal elastic oscillations leads to omitting the gyroscopic effects in the linearized form of in-plane motion. Similar results to those in Ref. 9 are also obtained for rigid body motion of a four-body system with different length configurations, which are not presented here.

Table 2 compares the nondimensional planar eigenfrequencies of different cases of a two-body tethered system obtained from the present formulation with those of Pasca and Pignataro.[12] Although the results are for two-body systems, there is, however, a very interesting point, showing the capabilities of the present formulation.

Because of some computing hardware restrictions the number of elastic modes of a tether in each direction was limited to two in the computation. It means that each tether at most can have six elastic degree of freedom. With this limitation, one can expect to obtain only the first two longitudinal and the first two transverse eigenfrequencies of the in-plane motion of a two-body system, and the higher frequencies of the system can not be obtained. Using what we call a segmented-tether model, i.e., by breaking the tethers to a number of smaller tethers and putting a negligible mass at the connection points of the smaller tethers, however, one can obtain the higher frequencies of the system to whatever order one desires, limited only by the capability of the computing facility being used.

Results of Ref. 12 and the present formulation, employing a segmented-tether model, for a two-body tethered system with tether density $\rho = 5.76$ kg/km, longitudinal stiffness $EA = 2.8 \times 10^5$ N, and different tether length and mass combinations are given in Table 2. The orbit is circular with orbital radius $R_c = 6657$ km. As an example, the two-body tethered system in the first case

Table 1 In-plane dimensionless frequencies (ω/Ω_c) of a three-body system

	Case 1: $\ell_1/\ell_2 = \frac{1}{5}$		Case 2: $\ell_1/\ell_2 = \frac{1}{3}$		Case 3: $\ell_1/\ell_2 = \frac{1}{1}$		
Mode	Present form.	Ref. 8	Present form.	Ref. 8	Present form.	Ref. 8	Type
1	1.725	1.732	1.725	1.732	1.724	1.732	Lib.
2	6.503	6.506	5.692	5.694	5.164	5.166	Lib
3	22.084	——	21.959	——	21.094	——	Long.
4	80.535	——	70.817	——	63.867	——	Long.
5	81.807	81.756	89.291	90.484	133.075	134.088	Tran.
6	161.131	162.917	178.665	180.366	146.909	147.642	Tran.
7	244.424	243.821	271.027	269.843	266.356	267.580	Tran.
8	322.178	326.062	278.702	279.322	294.268	295.183	Tran.

Table 2 In-plane dimensionless frequencies (ω/Ω_c) of a two-body system

	$\ell = 100$ km, $m_1 = 10^5$ kg $m_2 = 500$ kg		$\ell = 20$ km, $m_1 = \infty$ $m_2 = 576$ kg		$\ell = 20$ km, $m_1 = \infty$ $m_2 = 115.2$ kg		
Mode	Present form.	Ref. 12	Present form.	Ref. 12	Present form.	Ref. 12	Type
1	1.731	1.794	1.732	1.733	1.732	1.742	Lib.
2	6.389	6.905	12.777	12.780	6.709	6.750	Tran.
3	12.059	12.457	25.245	25.241	12.747	12.811	Tran.
4	17.879	18.269	37.795	37.771	18.929	19.014	Tran.
5	23.742	24.143	50.369	50.319	25.148	25.256	Tran.
10	53.344	53.807	—	—	—	—	Tran.
11	54.541	54.559	—	—	—	—	Long.
12	59.337	59.758	—	—	—	—	Tran.

Table 3 First 10 nondimensional longitudinal and transverse frequencies (ω/Ω_c) of a two-body TSS and an 11-body TSS

	Case 1: single-probe TSS $m_1 = 10^5$ kg, $m_2 = 500$ kg $\ell = 100$ km				Case 2: 10-probe TSS $m_1 = 10^5$ kg, $m_i = 500$ kg $\ell_1 = 55$ km, $\ell_i = 5$ km			
		Lib. and Tran.		$\frac{\omega_O^2 - \omega_I^2}{\Omega_c^2}$		Lib. and Tran.		$\frac{\omega_O^2 - \omega_I^2}{\Omega_c^2}$
Mode	Long.	ω_I	ω_O		Long.	ω_I	ω_O	
1	54.541	1.731	2.000	1.002	24.209	1.726	2.000	1.010
2	208.026	6.388	6.466	1.002	93.781	4.882	4.984	1.005
3	389.134	12.059	12.101	1.002	174.065	8.356	8.416	1.005
4	577.896	17.879	17.907	1.002	251.930	11.940	11.982	1.005
5	771.800	23.742	23.763	1.002	321.395	15.605	15.638	1.006
6	971.095	29.627	29.643	1.002	370.592	19.331	19.358	1.006
7	1176.628	35.528	35.542	1.002	412.193	23.039	23.061	1.007
8	1389.404	41.445	41.458	1.002	463.049	26.241	26.260	1.008
9	1610.410	47.383	47.393	1.002	508.205	28.699	28.716	1.008
10	1840.492	53.344	53.354	1.002	542.257	32.367	32.383	1.008

($\ell = 100$ km, $m_1 = 10^5$ kg, $m_2 = 500$ kg) is presented as a 21-body system with $m_1 = 10^5$ kg, $m_i = 0.001$ kg, $i = 2, \ldots, 20$; $m_{21} = 500$ kg, and $\rho_i = 5.76$ kg/km, $\ell_i = 5$ km, $i = 1, \ldots, 20$. In addition to three rigid DOFs, three elastic DOFs, one longitudinal, one in-plane transverse, and one out-of-plane transverse elastic DOF are considered for each tether. In total the system has 120 DOFs of which 20, corresponding to the tether lengths, are not involved in the eigenvalue problem since the system is in the stationkeeping phase. It takes only 80 s to find the fixed point and the eigenfrequencies of this system on a 486/66 personal computer.

The first column of Table 2 shows the mode number, whereas the last column represents the type of the modes. As can be seen, the results obtained in the two formulations for the second case ($\ell = 20$ km, $m_1 = \infty$, $m_2 = 576$ kg) are closer than the other two cases, because the parameter $\gamma = \rho\ell/m_2$ defined in Ref. 12, which has an important role in their theory and employed perturbation method, has a much lower value in this case than the other cases. As mentioned by the authors in Ref. 12, their results are more accurate for smaller γ.

Table 3 presents some results for a 10-probe tethered system deployed from the Shuttle and compares the first 10 longitudinal and the first 10 transverse frequencies with those of a single-probe case. The two-body system is exactly the same as the first case of Table 2. The multibody system consists of $m_1 = 10^5$ kg, $m_i = 500$ kg, $i = 2, \ldots, 11$; $\rho_i = 5.76$ kg/km, $EA_i = 2.8 \times 10^5$ N, $i = 1, \ldots, 10$; $\ell_1 = 55$ km, $\ell_i = 5$ km, $i = 2, \ldots, 10$. Thus, the total tether length is the same (100 km). Both systems have the same orbital motion. One can note many more low-frequency elastic modes for the 10-probe system. It is also noted that the in-plane and out-of-plane transverse frequencies are related by $(\omega_O/\Omega)_i^2 \approx (\omega_I/\Omega)_i^2 + 1$.

Numerical Simulations: System with Constant Lengths

Nonlinear equations of motion obtained from the present formulation have been integrated numerically using the Gear's method. For the three-body system, the results are the same as those obtained by Misra and Modi[9] and are omitted here for brevity. Dynamic response of a four-body system [tether elevator/crawler system or (TECS)] shown in Fig. 2, has also been obtained. This is discussed next.

A system similar to that studied by Cosmo et al.[7] is considered here, except that they have not considered transverse elastic oscillations of the tethers. The parameters of TECS are chosen as follows: $m_1 = 10^4$ kg, $m_2 = 3 \times 10^5$ kg, $m_3 = 5000$ kg, $m_4 = 10^4$ kg, $\ell_1 = 10.5$ km, $\ell_2 = 1$ km, $\ell_3 = 9$ km. The tethers have a linear mass density of $\rho_1 = \rho_2 = \rho_3 = 6$ kg/km and axial stiffness $EA_1 = EA_2 = EA_3 = 61575.2$ N. The system is in a circular orbit at an altitude of 450 km and is in the stationkeeping phase. The elastic oscillations of each tether are represented by 3 elastic DOFs, one longitudinal, one in-plane, and one out-of-plane transverse elastic mode. Therefore, the complete attitude motion of the system is described by 15 DOFs. The effect of structural damping on the response of the system is studied by introducing a damping ratio $\xi = 1.2\%$ based on the first natural frequency of the longitudinal elastic oscillation of the system.

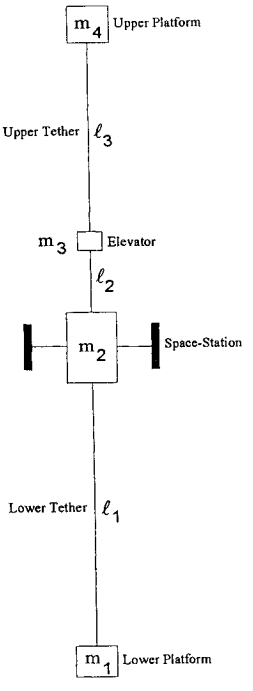

Fig. 2 Tether elevator/crawler system[4]: orbit radius R_c = 6828 km, lower platform mass m_1 = 10,000 kg, space station mass m_2 = 300,000 kg, elevator mass m_1 = 5000 kg, upper platform mass m_1 = 10,000 kg, tether mass density ρ = 6 kg/km, first tether length ℓ_1 = 10.5 km, second tether length ℓ_2 = 1 km, third tether length ℓ_3 = 9 km, tether stiffness EA = 61,575 N, and structural damping ζ = 1.2%.

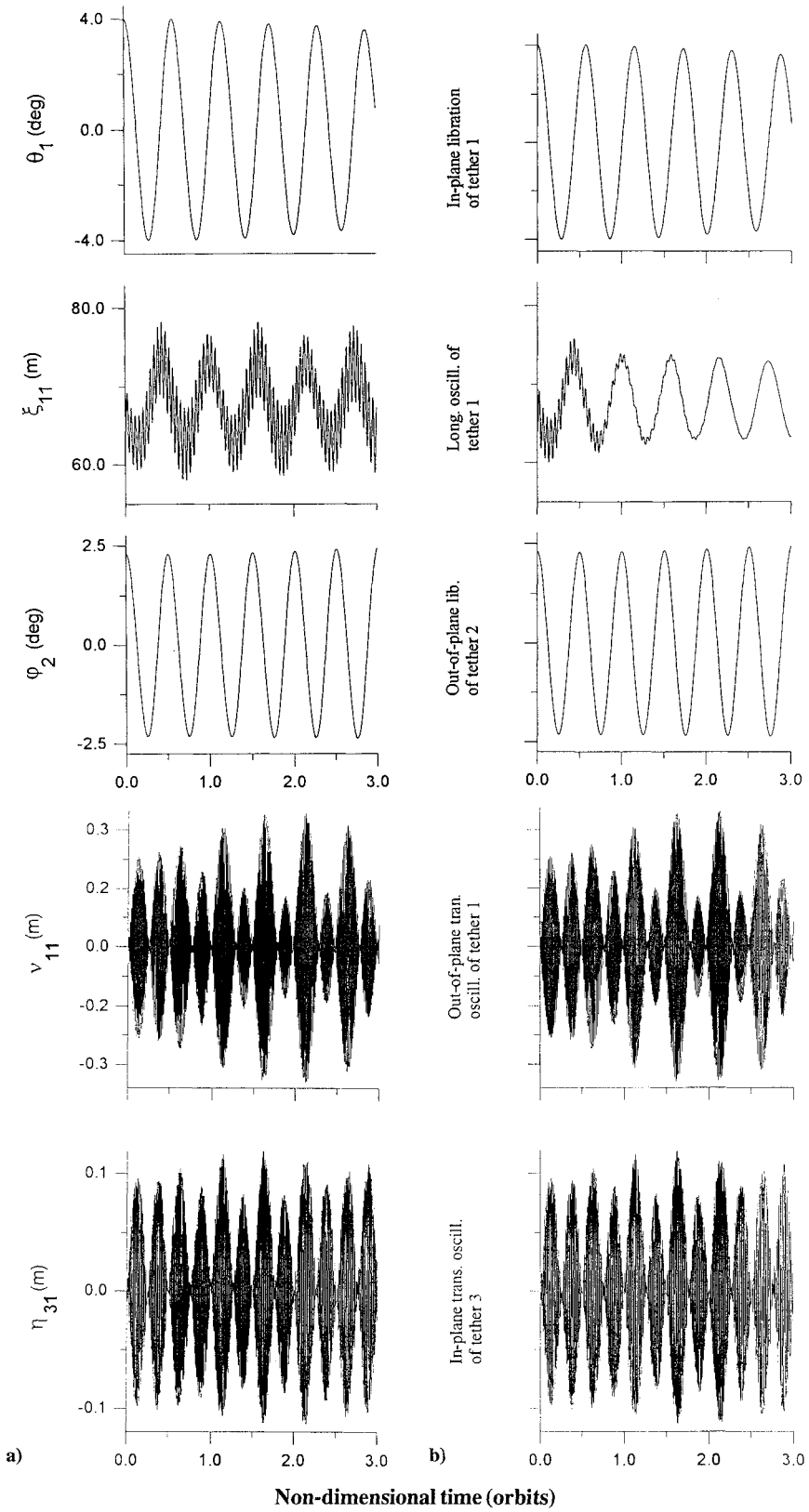

Fig. 3 Typical dynamic response of TECS with constant length a) in the absence of material damping and b) in the presence of material damping.

Table 4 presents the eigenvalues of the TECS, in the absence and presence of structural damping of the tethers. At the bottom, the longitudinal stretches of the tethers in the equilibrium position of the system are given. The structural damping affects the longitudinal modes directly but the librational motion as well as the transverse modes only through a second-order coupling. Thus, the eigenvalues associated with the transverse oscillations have much smaller damping (negative real parts). This can be also observed in the dynamical response of the system (Fig. 3). Note that the structural damping introduces no damping to the out-of-plane frequencies (Table 4). That is because the in-plane (IP) and out-of-plane (OP) motion are decoupled in the linear sense. One can also notice that the structural damping here has almost no effect on the natural frequencies of the system (imaginary parts) but has a significant effect on the real parts of the eigenvalues associated with the higher modes of the system.

Simulation up to 17,000 s (~3 orbits) of the stationkeeping phase of TECS has been run with a set of initial conditions that perturb the

system from its equilibrium position and excite its general dynamics. The initial conditions were chosen as follows, where values for θ and ϕ are in radians (degrees) and for ξ, η, ν are in meters:

$$\theta_1 = 0.07(4.01), \quad \phi_1 = 0.05(2.86), \quad \xi_{11} = 64.0$$
$$\eta_{11} = 10.0, \quad \nu_{11} = 0.0, \quad \theta_2 = 0.04(2.29)$$
$$\phi_2 = 0.03(1.72), \quad \xi_{21} = 6.0, \quad \eta_{21} = \nu_{21} = 0.0$$
$$\theta_3 = 0.04(2.29), \quad \phi_3 = 0.03(1.72), \quad \xi_{31} = 52.0$$
$$\eta_{31} = 0.0, \quad \nu_{31} = 5.0$$

Figure 3 shows the time history of some of the generalized coordinates of the system in the absence and presence of the structural damping. The effect of structural damping in the longitudinal oscillations of the tethers is quite evident (second graph in Figs. 3a and 3b). As has been said before, however, it has almost no effect on the librational and transverse oscillations of the tethers.

Numerical Simulations: System with Variable Lengths

Figures 4 and 5 display simulation results up to 18 orbits for librational motion and 2.5 orbits for vibrational motion of the tethers for a two-phase operation: deployment of the elevator in approximately one orbit followed by the stationkeeping phase. The elevator (m_3) is deployed from the space station by increasing the second tether length. The following strategy is used for this operation:

$$\ell_2 = (\ell_2)_0 + \frac{\Delta\ell_2}{T}\left[t - \frac{T}{2\pi}\sin\left(\frac{2\pi t}{T}\right)\right] \qquad t \le T$$
$$\ell_2 = (\ell_2)_f = (\ell_2)_0 + \Delta\ell_2 \qquad t > T \qquad (32)$$
$$m_2 = (m_2)_0 - \rho_2[\ell_2 - (\ell_2)_0]$$

where $(\ell_2)_0 = 1$ km, $\Delta\ell_2 = 9$ km, and $T = 5600$ s for the present case. The same parameters are chosen as in the stationkeeping phase using the same units, and the initial conditions are set as follows:

$$\theta_1 = 0.07(4.01), \quad \phi_1 = 0.05(2.86), \quad \xi_{11} = 64.0$$
$$\eta_{11} = 50.0, \quad \nu_{11} = 10.0, \quad \theta_2 = 0.04(2.29)$$
$$\phi_2 = 0.03(1.72), \quad \xi_{21} = 6.0, \quad \eta_{21} = 10.0$$
$$\nu_{21} = 5.0, \quad \theta_3 = 0.04(2.29), \quad \phi_3 = 0.03(1.72)$$
$$\xi_{31} = 52.0, \quad \eta_{31} = 50.0, \quad \nu_{31} = 10.0$$

Table 4 Eigenvalues and nominal stretch of the tethers of TECS

Mode	In the absence of structural damping	In the presence of structural damping	Type
	System eigenvalues		
1	$0 \pm 1.7247i$	$-0.00001 \pm 1.7247i$	IP lib.
2	$0 \pm 1.7839i$	$-0.00001 \pm 1.7839i$	IP lib.
3	$0 \pm 2.0000i$	$0 \pm 2.0000i$	OP lib.
4	$0 \pm 2.0512i$	$0 \pm 2.0512i$	OP lib.
5	$0 \pm 8.4160i$	$-0.00001 \pm 8.4160i$	IP lib.
6	$0 \pm 8.4768i$	$0 \pm 8.4768i$	OP lib.
7	$0 \pm 21.7990i$	$-0.26528 \pm 21.7974i$	Long.
8	$0 \pm 22.7067i$	$-0.28789 \pm 22.7048i$	Long.
9	$0 \pm 68.8932i$	$0 \pm 68.8932i$	IP tran.
10	$0 \pm 68.9004i$	$0 \pm 68.9004i$	OP tran.
11	$0 \pm 78.4984i$	$-0.00000 \pm 78.4984i$	IP tran.
12	$0 \pm 78.5047i$	$0 \pm 78.5047i$	OP tran.
13	$0 \pm 105.3134i$	$-6.20478 \pm 105.1304i$	Long.
14	$0 \pm 723.1814i$	$0 \pm 723.1814i$	IP tran.
15	$0 \pm 723.1821i$	$0 \pm 723.1821i$	OP tran.

Tether stretches: $u_{\ell_1} = 67.835$ m, $u_{\ell_2} = 6.464$ m, $u_{\ell_3} = 55.351$ m

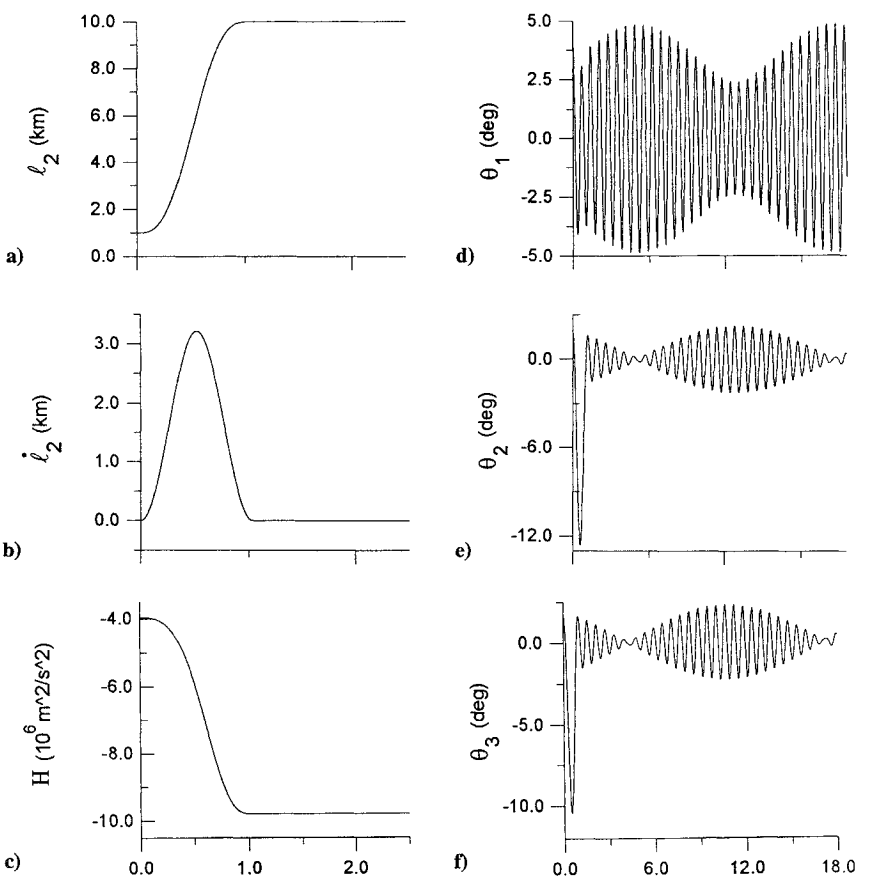

Fig. 4 Typical dynamic response of TECS with variable length: a) length variation of tether 2, b) deployment rate of tether 2, c) Hamiltonian of the system, d) in-plane libration of the tether 1, e) in-plane libration of the tether 2, and f) in-plane libration of the tether 3.

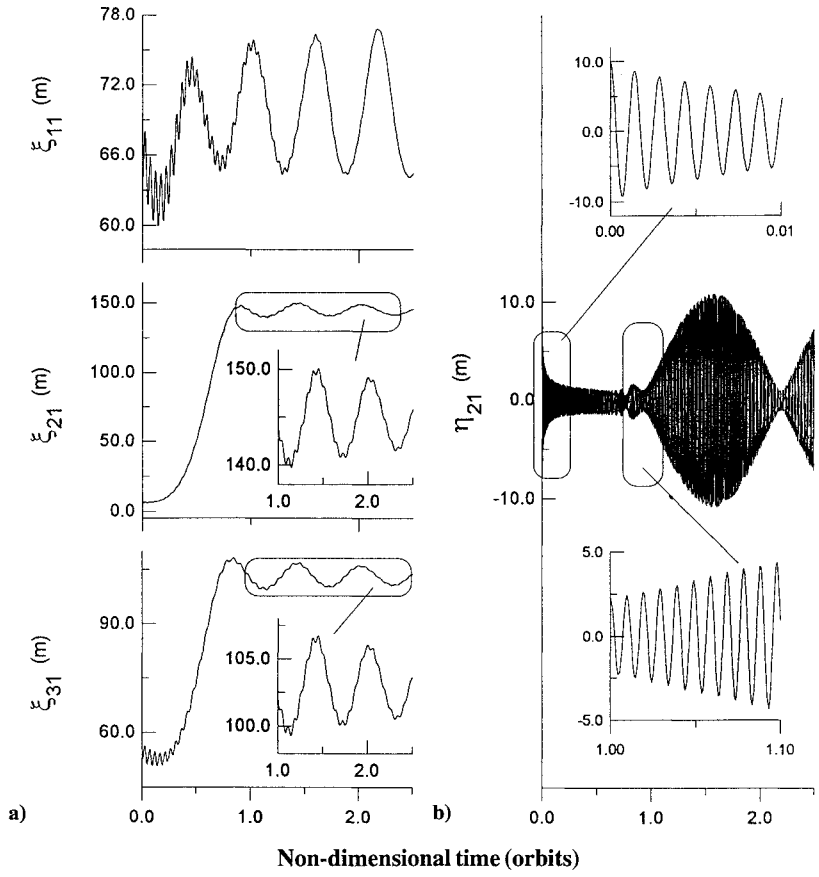

Fig. 5 Typical dynamic response of TECS with variable length: a) longitudinal oscillation of the tethers and b) in-plane transverse oscillation of tether 2.

The deployment strategy is shown in Figs. 4a and 4b, and the Hamiltonian of the system is shown in Fig. 4c. Note that during the stationkeeping phase the Hamiltonian is conserved, which gives some confidence in the formulation and numerical analysis. Comparing the results shown in Figs. 4 and 5, one can see that the deployment here has a greater effect on the librational and vibrational motion of tethers 2 and 3 than on the first tether. This can be explained by a very small effect of deployment on the position of the center of mass and, consequently, on that of the lower platform. The Coriolis effect on the librational motions can be seen clearly from Figs. 4d–4f. These figures show that during the accelerating period these motions tend to grow, whereas it is the converse for the decelerating period. Therefore, it is evident that the librational motion can become unstable, even in deployment phase, for a particular range of deploying rate. Because of the very close librational frequencies of the system in the final stationkeeping phase, there is a beat phenomenon between the librational motion of the first tether and the other two tethers that can be seen in Figs. 4d–4f.

Figure 5a shows the longitudinal oscillations of the tethers. It is seen that during the deployment, the longitudinal stretch of tethers 2 and 3 are affected more than that of tether 1. This is because of increasing tension in these two tethers due to deployment of m_3 and m_4 to higher altitudes. Typical transverse vibrations of the tethers, usually oscillatory motions with high frequency, are shown in Fig. 5b. The shorter the tether length, the higher is the frequency.

Conclusions

A Lagrangian formulation for three-dimensional motion of N-body tethered systems was presented. The equations of motion obtained are valid for large motion, variable lengths, flexible and massive tethers, and any arbitrary orbit. The continuous tethers were discretized using the assumed-mode method. The nonlinear equations of motion were linearized analytically for stability analysis and control applications. Eigenvalue analysis was carried out for several multibody tethered systems in the stationkeeping phase. The segmented-tether model was introduced to obtain higher natural frequencies of the system. It was observed that for small motion the out-of-plane frequencies ω_{O_j} are, in general, related to the in-plane frequencies by the approximate relation $\omega_{O_j}^2 \approx \omega_{I_j}^2 + \Omega_c^2$, Ω_c being the orbital frequency. It can be explained by the fact that the sum of the gravity gradient and the centrifugal gadient is proportional to $4\Omega_c^2$ for the out-of-plane displacements and equal to $3\Omega_c^2$ for the in-plane displacements.

Typical transient response of a four-body tethered system, called TECS, was presented for two different cases: constant length and variable length. The effect of structural damping on the eigenvalues of the system and its uncontrolled motion was studied. It was noticed that this damping has a negligible effect on the transverse oscillations of the tethers, whereas their longitudinal oscillations are significantly affected.

The formulation presented here would be useful for the dynamical and control analysis of multiprobe systems, as well as for possible space-station-based tethered systems.

Appendix A: Explicit Expressions for Various Terms in Eq. (20)

The terms ${}_pG_{njk}$, ${}_pH_{nj}$, ${}_pP_{nj}$, and ${}_pS_n$ appearing in Eq. (20) are given by

$$
\begin{aligned}
{}_pG_{njk} = \frac{\partial B_n}{\partial_p q_n}\Bigg\{\Bigg[\bar{\mu}_j\big(\ddot{\boldsymbol{b}}_j + \alpha_0^2\{\boldsymbol{b}_j - 3(\hat{\boldsymbol{i}}_c\cdot\boldsymbol{b}_j)\hat{\boldsymbol{i}}_c\}\big) \\
- (2\dot{B}_j\dot{\boldsymbol{r}}_j + \ddot{B}_j\boldsymbol{r}_j) - A_{nj}\ddot{\boldsymbol{r}}_j - \frac{\alpha_0^2}{2}(2A_{nj} - \delta_{nj}) \\
\times\{\boldsymbol{r}_j - 3(\hat{\boldsymbol{i}}_c\cdot\boldsymbol{r}_j)\hat{\boldsymbol{i}}_c\}\Bigg]\cdot\boldsymbol{r}_n + \frac{1}{2}\delta_{nj}\dot{\boldsymbol{r}}_j\cdot\dot{\boldsymbol{r}}_n\Bigg\}
\end{aligned}
\tag{A1}
$$

$$
{}_pH_{nj} = [-\dot{B}_j(2A_{jn} + \delta_{jn})\dot{\boldsymbol{r}}_j + 2\bar{\mu}_j\dot{B}_n\dot{\boldsymbol{b}}_j - A_{jn}\ddot{B}_j\boldsymbol{r}_j]\cdot\frac{\partial\boldsymbol{r}_n}{\partial_p q_n}
\tag{A2}
$$

$$
{}_pP_{nj} = \left(F_{jn}\frac{\partial \boldsymbol{r}_n}{\partial_p q_n} + \bar{\mu}_n A_{nj}\frac{\partial \boldsymbol{b}_n}{\partial_p q_n}\right)\cdot\left[\ddot{\boldsymbol{r}}_j + \alpha_0^2(\boldsymbol{r}_j - 3(\hat{\boldsymbol{i}}_c\cdot\boldsymbol{r}_j)\hat{\boldsymbol{i}}_c)\right]
$$

$$
+\left(\bar{\mu}_j A_{jn}\frac{\partial \boldsymbol{r}_n}{\partial_p q_n} - \bar{\mu}_j\bar{\mu}_n\frac{\partial \boldsymbol{b}_n}{\partial_p q_n}\right)\cdot\left[\ddot{\boldsymbol{b}}_j + \alpha_0^2(\boldsymbol{b}_j - 3(\hat{\boldsymbol{i}}_c\cdot\boldsymbol{b}_j)\hat{\boldsymbol{i}}_c)\right] \tag{A3}
$$

$$
{}_pS_n = \hat{\rho}_n\int_0^{\ell_n}\left(\ddot{\boldsymbol{r}}_{t_n} + \alpha_0^2\left\{\boldsymbol{r}_{t_n} - 3\left(\hat{\boldsymbol{i}}_c\cdot\boldsymbol{r}_{t_n}\right)\hat{\boldsymbol{i}}_c\right\}\cdot\frac{\partial \boldsymbol{r}_{t_n}}{\partial_p q_n}\,\mathrm{d}x_n\right.
$$

$$
+\dot{B}_n\dot{\boldsymbol{r}}_n\cdot\frac{\partial \boldsymbol{r}_n}{\partial_p q_n} + \frac{EA_n}{2m}\int_0^{\ell_n}\frac{\partial \mathcal{E}_n}{\partial_p q_n}\,\mathrm{d}x_n + {}_pL_n \tag{A4}
$$

where ${}_pL_n = 0$ for ${}_pq_n \neq \ell_n$ and

$$
{}_pL_n = \frac{EA_n}{2m}(\mathcal{E}_n)_{x_n=\ell_n} + \hat{\rho}_n\left(\alpha_n - \frac{1}{2}\right)\left[\dot{\boldsymbol{r}}_{t_n}\cdot\dot{\boldsymbol{r}}_{t_n}\right]_{x_n=0} \tag{A5}
$$

for ${}_pq_n = \ell_n$. In the above equations $\mathcal{E}_n$ is defined as

$$
\mathcal{E}_i = \left\{\frac{\partial u_i}{\partial x_i} + \frac{1}{2}\left[\left(\frac{\partial v_i}{\partial x_i}\right)^2 + \left(\frac{\partial w_i}{\partial x_i}\right)^2\right]\right\}^2
$$

$$
-\left(\frac{\partial u_i}{\partial x_i}\right)^2\left[\left(\frac{\partial u_i}{\partial x_i}\right)^2 + \left(\frac{\partial w_i}{\partial x_i}\right)^2\right] \tag{A6}
$$

Appendix B: Quantities Required to Evaluate $\ddot{\boldsymbol{r}}_j$, $\ddot{\boldsymbol{b}}_j$, and $\ddot{\boldsymbol{r}}_{t_j}$

Defining the following expressions:

$$
\boldsymbol{X}_{*i} = \int_0^1 \boldsymbol{X}_i\,\mathrm{d}s_i, \qquad \boldsymbol{X}_i' = \frac{\mathrm{d}\boldsymbol{X}_i}{\mathrm{d}s_i}, \qquad \boldsymbol{X}_i'' = \frac{\mathrm{d}^2\boldsymbol{X}_i}{\mathrm{d}s_i^2}
$$

$$
\boldsymbol{Y}_{*i} = \int_0^1 \boldsymbol{Y}_i\,\mathrm{d}s_i, \qquad \boldsymbol{Y}_i' = \frac{\mathrm{d}\boldsymbol{Y}_i}{\mathrm{d}s_i}, \qquad \boldsymbol{Y}_i'' = \frac{\mathrm{d}^2\boldsymbol{Y}_i}{\mathrm{d}s_i^2} \tag{B1}
$$

$$
\boldsymbol{Z}_{*i} = \int_0^1 \boldsymbol{Z}_i\,\mathrm{d}s_i, \qquad \boldsymbol{Z}_i' = \frac{\mathrm{d}\boldsymbol{Z}_i}{\mathrm{d}s_i}, \qquad \boldsymbol{Z}_i'' = \frac{\mathrm{d}^2\boldsymbol{Z}_i}{\mathrm{d}s_i^2}
$$

where $s_i = x_i/\ell_i$ and vectors

$$
\boldsymbol{\Lambda}_i = [\dot{\phi}_i(\dot{\theta}_0 + \dot{\theta}_i)\cos\phi_i + \ddot{\theta}_0\sin\phi_i]\hat{\boldsymbol{i}}_i
$$

$$
+[-\dot{\phi}_i(\dot{\theta}_0 + \dot{\theta}_i)\sin\phi_i + \ddot{\theta}_0\cos\phi_i]\hat{\boldsymbol{k}}_i
$$

$$
\boldsymbol{\gamma}_i = \sin\phi_i\hat{\boldsymbol{i}}_i + \cos\phi_i\hat{\boldsymbol{k}}_i
$$

$$
\boldsymbol{\Omega}_i = (\Omega_c + \dot{\theta}_i)\sin\phi_i\hat{\boldsymbol{i}}_i - \dot{\phi}_i\hat{\boldsymbol{j}}_i + (\Omega_c + \dot{\theta}_i)\cos\phi_i\hat{\boldsymbol{k}}_i
$$

$$
\boldsymbol{\sigma}_i = \dot{\phi}_i(\cos\phi_i\hat{\boldsymbol{i}}_i - \sin\phi_i\hat{\boldsymbol{k}}_i) \tag{B2}
$$

$$
\boldsymbol{\zeta}_i = \boldsymbol{X}_i^T\dot{\boldsymbol{\xi}}_i\hat{\boldsymbol{i}}_i + \boldsymbol{Y}_i^T\dot{\boldsymbol{\eta}}_i\hat{\boldsymbol{j}}_i + \boldsymbol{Z}_i^T\dot{\boldsymbol{\nu}}_i\hat{\boldsymbol{k}}_i
$$

$$
\boldsymbol{\zeta}_{*i} = \boldsymbol{X}_{*i}^T\dot{\boldsymbol{\xi}}_i\hat{\boldsymbol{i}}_i + \boldsymbol{Y}_{*i}^T\dot{\boldsymbol{\eta}}_i\hat{\boldsymbol{j}}_i + \boldsymbol{Z}_{*i}^T\dot{\boldsymbol{\nu}}_i\hat{\boldsymbol{k}}_i
$$

$$
\boldsymbol{\varsigma}_i = \boldsymbol{X}_i'^T\boldsymbol{\xi}_i\hat{\boldsymbol{i}}_i + \boldsymbol{Y}_i'^T\boldsymbol{\eta}_i\hat{\boldsymbol{j}}_i + \boldsymbol{Z}_i'^T\boldsymbol{\nu}_i\hat{\boldsymbol{k}}_i
$$

$$
\boldsymbol{\varrho}_i = \boldsymbol{X}_i''^T\boldsymbol{\xi}_i\hat{\boldsymbol{i}}_i + \boldsymbol{Y}_i''^T\boldsymbol{\eta}_i\hat{\boldsymbol{j}}_i + \boldsymbol{Z}_i''^T\boldsymbol{\nu}_i\hat{\boldsymbol{k}}_i
$$

then vectors $\boldsymbol{d}_{r_i}$, $\boldsymbol{d}_{b_i}$, $\boldsymbol{d}_{t_i}$ are given by

$$
\boldsymbol{d}_{r_i} = 2\boldsymbol{\Omega}_i\times\mathring{\boldsymbol{r}}_i + \boldsymbol{\Omega}_i\times(\boldsymbol{\Omega}_i\times\boldsymbol{r}_i) + \boldsymbol{\Lambda}_i\times\boldsymbol{r}_i
$$

$$
\boldsymbol{d}_{b_i} = \left(\dot{\ell}_i^2/\ell_0\right)\hat{\boldsymbol{i}}_i + (2\dot{\ell}_i/\ell_0)\boldsymbol{\zeta}_{*i} + 2\boldsymbol{\Omega}_i\times\mathring{\boldsymbol{b}}_i
$$

$$
+\boldsymbol{\Omega}_i\times(\boldsymbol{\Omega}_i\times\boldsymbol{b}_i) + \boldsymbol{\Lambda}_i\times\boldsymbol{b}_i \tag{B3}
$$

$$
\boldsymbol{d}_{t_i} = (-2\dot{s}_i\dot{\ell}_i/\ell_i)\boldsymbol{\varsigma}_i + \dot{s}_i^2\boldsymbol{\varrho}_i + 2\dot{s}_i\boldsymbol{\zeta}_i + 2\boldsymbol{\Omega}_i\times\mathring{\boldsymbol{r}}_{t_i}
$$

$$
+\boldsymbol{\Omega}_i\times\left(\boldsymbol{\Omega}_i\times\boldsymbol{r}_{t_i}\right) + \boldsymbol{\Lambda}_i\times\boldsymbol{r}_{t_i}
$$

The column vectors $\mathcal{D}_{r_i}$, $\mathcal{D}_{b_i}$, and $\mathcal{D}_{t_i}$ are, in fact, partial derivatives of vectors $\boldsymbol{r}_i$, $\boldsymbol{b}_i$, and $\boldsymbol{r}_{t_i}$ with respect to the elements of generalized coordinate vector $\boldsymbol{q}_i$ corresponding to the ith tether, respectively. They are given by

$$
\mathcal{D}_{r_i} = \begin{Bmatrix} \boldsymbol{\gamma}_i\times\boldsymbol{r}_i \\ -\hat{\boldsymbol{j}}_i\times\boldsymbol{r}_i \\ \hat{\boldsymbol{i}}_i \\ \boldsymbol{X}_{\ell_i}\hat{\boldsymbol{i}}_i \\ \boldsymbol{0} \\ \boldsymbol{0} \end{Bmatrix}, \qquad \mathcal{D}_{b_i} = \begin{Bmatrix} \boldsymbol{\gamma}_i\times\boldsymbol{b}_i \\ -\hat{\boldsymbol{j}}_i\times\boldsymbol{b}_i \\ \dfrac{1}{\ell_i}\boldsymbol{b}_i + \dfrac{\ell_i}{2\ell_0}\hat{\boldsymbol{i}}_i \\ \ell_i\boldsymbol{X}_{*i}\hat{\boldsymbol{i}}_i/\ell_0 \\ \ell_i\boldsymbol{Y}_{*i}\hat{\boldsymbol{j}}_i/\ell_0 \\ \ell_i\boldsymbol{Z}_{*i}\hat{\boldsymbol{k}}_i/\ell_0 \end{Bmatrix}
$$

$$
\mathcal{D}_{t_i} = \begin{Bmatrix} \boldsymbol{\gamma}_i\times\boldsymbol{r}_{t_i} \\ -\hat{\boldsymbol{j}}_i\times\boldsymbol{r}_{t_i} \\ \boldsymbol{i}_i + \dfrac{1-s_i}{\ell_i}\boldsymbol{\varsigma}_i \\ \boldsymbol{X}_i\hat{\boldsymbol{i}}_i \\ \boldsymbol{Y}_i\hat{\boldsymbol{j}}_i \\ \boldsymbol{Z}_i\hat{\boldsymbol{k}}_i \end{Bmatrix}
$$

Acknowledgments

The authors gratefully acknowledge the support given to this research by the Natural Sciences and Engineering Research Council of Canada. The first author also acknowledges the scholarship provided by the Ministry of Higher Education of the Islamic Republic of Iran and a Major Fellowship awarded by the Faculty of Graduate Studies and Research of McGill University. This work was presented as Paper 93-700 at the AAS/AIAA Astrodynamics Conference, Victoria, British Columbia, Canada, Aug. 16–19, 1993.

References

[1]Misra, A. K., and Modi, V. J., "A Survey on the Dynamics and Control of the Tethered Satellite Systems," *Advances in the Astronautical Sciences*, Vol. 62, 1987, pp. 667–719.

[2]Anon., *Tethers in Space Handbook*, NASA Office of Space Flight, Advanced Program Development, Washington, DC, May 1989.

[3]Beletsky, V. V., and Levin, E. M., "Dynamics of Space Tether Systems," *Advances in the Astronautical Sciences*, Vol. 83, 1993.

[4]Lorenzini, E. C., "A Three-Mass Tethered System for Micro-*g*/Variable-*g* Applications," *Journal of Guidance, Control, and Dynamics*, Vol. 10, No. 3, 1987, pp. 242–249.

[5]Misra, A. K., Amier, Z. E., and Modi, V. J., "Attitude Dynamics of Three-Body Tethered Systems," *Acta Astronautica*, Vol. 17, No. 10, 1988, pp. 1059–1068.

[6]Lorenzini, E. C., Cosmo, M., Vetrella, S., and Moccia, A., "Acceleration Levels on Board the Space Station and a Tethered Elevator for Micro and Variable-Gravity Applications," *Proceeding of the NASA/PSN/AIAA Second International Conference on Tethers in Space* (Venice, Italy), 1987, pp. 513–522.

[7]Cosmo, M., Lorenzini, E. C., Vetrella, S., and Moccia, A., "Transient Dynamics of the Tether Elevator/Crawler System," *Proceeding of the AIAA/ASS Astrodynamics Conference* (Minneapolis, MN), 1988, pp. 480–489.

[8]Kumar, K., Jha, O. N., Misra, A. K., and Yan, Y., "Transverse Elastic Oscillations of Three-Body Tethered Systems," *Advances in the Astronautical Sciences*, Vol. 76, 1991, pp. 2383–2396.

[9]Misra, A. K., and Modi, V. J., "Three-Dimensional Dynamics and Control of Tether-Connected *N*-Body Systems," *Acta Astronautica*, Vol. 26, 1992, pp. 77–84.

[10]Onada, J., and Watanabe, N., "Tethered Subsatellite Swinging from Atmospheric Gradient," *Journal of Guidance, Control, and Dynamics*, Vol. 11, No. 5, 1988, pp. 477–479.

[11]Keshmiri, M., and Misra, A. K., "Effects of Aerodynamic Lift on the Stability of Tethered Subsatellite Systems," AAS/AIAA Spaceflight Mechanics Meeting, Pasadena, CA, AAS Paper 93-184, Feb. 1993.

[12]Pasca, M., and Pignataro, M., "Three-Dimensional Vibrations of Tethered Satellite Systems," *Journal of Guidance, Control, and Dynamics*, Vol. 14, No. 2, 1991, pp. 312–320.